

# Asymmetric Supramolecular Primary Amine Catalysis in Aqueous Buffer: Connections of Selective Recognition and Asymmetric Catalysis

Shenshen Hu, Jiuyuan Li, Junfeng Xiang, Jie Pan, Sanzhong Luo,\* and Jin-Pei Cheng\*

Beijing National Laboratory for Molecular Sciences (BNLMS), CAS Key Laboratory of Molecular Recognition and Function, Institute of Chemistry, Chinese Academy of Sciences, Beijing, 100190, China

Received April 5, 2010; E-mail: luosz@iccas.ac.cn; chengjp@most.cn

**Abstract:** A new approach of asymmetric supramolecular catalysis has been developed by combining the supramolecular recognition of  $\beta$ -cyclodextrin ( $\beta$ -CD) and the superior property of a chiral primary amine catalyst. The resulted  $\beta$ -CD enamine catalysts could effectively promote asymmetric direct aldol reactions with excellent enantioselectivity in an aqueous buffer solution (pH = 4.80). The identified optimal catalyst **CD-1** shows interesting characteristics of supramolecular catalysis with selective recognition of aldol acceptors and donors. A detailed mechanistic investigation on such supramolecular catalysis was conducted with the aid of NMR, fluorescence, circular dichroism, and ESI-MS analysis. It is revealed that the reaction is initialized first by binding substrates into the cyclodextrin cavity via a synergistic action of hydrophobic interaction and noncovalent interaction with the **CD-1** side chain. A rate-limiting enamine forming step is then involved which is followed by the product-generating C–C bond formation. A subsequent product release from the cavity completes the catalytic cycle. The possible connections between molecular recognition and asymmetric catalysis as well as their relevance to enamine catalysis in both natural enzymes and organocatalysts are discussed based on rational analysis.

## Introduction

Reaction pockets are ubiquitous in enzymes, wherein superb stereocontrol and catalytic efficiency are achieved by catching substrates in a beneficial orientation and conformation and by stabilizing the transition state.<sup>1</sup> Inspired by Nature, the construction of various supramolecular hosts, either synthetic or natural, to mimic the catalysis of enzymes has been the subject of intensive research for decades in supramolecular chemistry.<sup>2</sup> While remarkable acceleration in reactivity and improvement of regioselectivity have been achieved in many reactions via supramolecular strategy/approaches,<sup>3</sup> there are a less number of reports on enantioselective supramolecular catalysis, particularly those related to biomimetic asymmetric catalysts that could work favorably under normal enzymatic conditions.<sup>4</sup> The reason may be due to the usually nontrivial synthetic efforts in constructing the chiral supramolecular systems as well as the frequently encountered failures in converting the exquisite recognition properties of the deliberately designed host–guest system into catalytic turnovers.<sup>5</sup> Clearly, the delicate balance between recognition and catalysis, which has been practiced in

nature for billions of years, is still poorly understood in the context of supramolecular systems. To elucidate the possible connections between recognition and chiral catalysis with a simple supramolecule-linked asymmetric catalyst will certainly shed new light on supramolecular catalyst design and strengthen our understanding of enzymatic catalysis as well.

Herein, we present the first example of asymmetric supramolecular primary amine catalysts that promote direct aldol reactions with high efficiency and stereoselectivity in aqueous buffer (pH = 4.80). With a quite straightforward strategy, a simple and naturally occurring chiral host, i.e.  $\beta$ -cyclodextrin, is endowed with proven organocatalytic motifs<sup>6</sup> and such a marriage resulted in a viable approach that enabled efficient asymmetric supramolecular catalysis beyond the reach of small

- (1) (a) Kirby, A. J. *Angew. Chem., Int. Ed. Engl.* **1996**, *35*, 706–724. (b) Cacciapaglia, R.; Di Stefano, S.; Mandolini, L. *Acc. Chem. Res.* **2004**, *37*, 113–122. (c) Ringe, D.; Petsko, G. A. *Science* **2008**, *320*, 1428–1429.
- (2) (a) van Leeuwen, P. W. N. M., Ed. *Supramolecular Catalysis*; Wiley-VCH: Weinheim, 2008. (b) Breslow, R., Ed.; *Artificial enzyme*; Wiley-VCH: Weinheim, 2005. (c) Pluth, M. D.; Bergman, R. G.; Raymond, K. N. *Acc. Chem. Res.* **2009**, *42*, 1650–1659. (d) Rebek, J. J. *Acc. Chem. Res.* **2009**, *42*, 1660–1668.

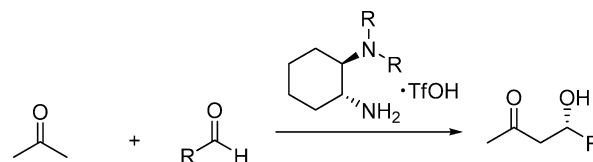
- (3) For recent examples of achiral supramolecular host–guest catalysis, see: (a) Klöck, C.; Dsouza, R. N.; Nau, W. N. *Org. Lett.* **2009**, *12*, 2595–2598. (b) Pinacho Crisóstomo, F. R.; Lledó, A.; Shenoy, S. R.; Iwasawa, T.; Rebek, J. J. *J. Am. Chem. Soc.* **2009**, *131*, 7402–7410. (c) Yebeutchou, R. M.; Dalcanele, E. *J. Am. Chem. Soc.* **2009**, *131*, 2452–2453. (d) Kumar, V. P.; Reddy, V. P.; Sridhar, R.; Srinivas, B.; Narender, M.; Rao, K. R. *J. Org. Chem.* **2008**, *73*, 1646–1648. (e) Pluth, M. D.; Bergman, R. G.; Raymond, K. N. *J. Org. Chem.* **2009**, *74*, 58–63. (f) Hastings, C. J.; Fiedler, D.; Bergman, R. G.; Raymond, K. N. *J. Am. Chem. Soc.* **2008**, *130*, 10977–10983. (g) Pluth, M. D.; Bergman, R. G.; Raymond, K. N. *J. Org. Chem.* **2009**, *74*, 58–63. (h) Das, S.; Brudvig, G. W.; Crabtree, R. H. *Chem. Commun.* **2008**, 413–424. (i) Fenger, T. H.; Marinescu, L. G.; Bols, M. *Org. Biomol. Chem.* **2009**, *7*, 933–943. (j) Pluth, M. D.; Bergman, R. G.; Raymond, K. N. *J. Am. Chem. Soc.* **2008**, *130*, 11423–11429. (k) Cafeo, G.; Kohnke, F. H.; Valenti, L. *Tetrahedron Lett.* **2009**, *50*, 4138–4140. (l) Shenoy, S. R.; Pinacho Crisóstomo, F. R.; Iwasawa, T.; Rebek, J. J. *J. Am. Chem. Soc.* **2008**, *130*, 5658–5659.

molecules. Moreover, systematic mechanism studies with the aid of typical host–guest analyzing techniques such as X-ray crystallography, NMR, UV, CD, and fluorescence spectroscopy reveal some catalytic features resembling those of the enzyme catalysis: (1) substrates binding *via* cooperative noncovalent interactions such as hydrophobic effect, hydrogen bonding, or electrostatic interaction; (2) recognition induced conformation changes of the host molecule that favor the catalysis; and (3) stereocontrol *via* synergistic interactions of chiral host and side chains. The details of the mechanism studies as well as the synthetic scopes and limitations of the current asymmetric supramolecular catalyst are also presented.

## Results and Discussions

**1. Design and Synthesis of Catalysts.** Simple chiral primary amines (e.g., **7**) have recently been reported to serve as efficient enamine-type catalysts that mechanistically and functionally resemble the lysine-based aldolases (Scheme 1).<sup>7</sup> It is envisioned that efficient and biomimetic asymmetric supramolecular catalysis may be evolved by covalently connecting the established primary aminocatalytic motif with a chiral supramolecular host. To achieve this, we have chosen the simple natural cyclodextrins (CD) among several prominent supramolecular hosts. This

**Scheme 1.** Chiral Primary Amine Catalyzed Asymmetric Direct Aldol Reactions



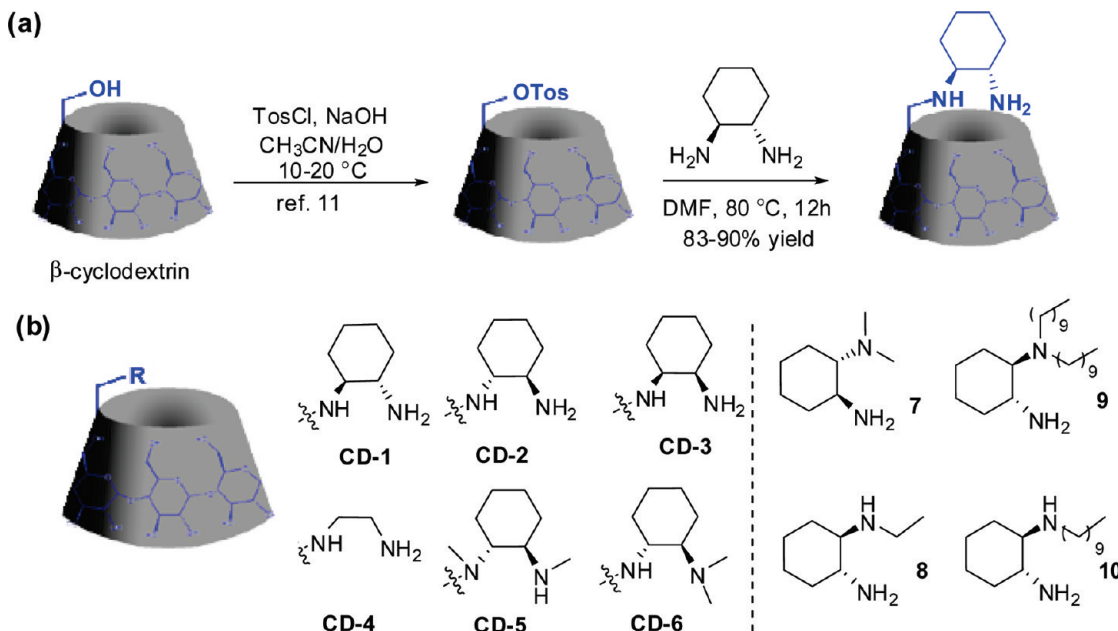
design is based on the considerations that (1) cyclodextrins are readily available and have been extensively explored as enzymatic mimics in aqueous buffer;<sup>8</sup> (2) in particular, cyclodextrin derivatives have already been examined as enamine or enol-based aldolase mimics;<sup>9</sup> (3) moreover, native cyclodextrins together with derivatives have been proven to be feasible asymmetric catalysts in photocatalytic reactions with moderate to high enantioselectivity;<sup>4f,j,l,17b,c</sup> and (4) recently, the use of cyclodextrins as an immobilizing host in asymmetric aldol catalysis has also been attempted in a few studies.<sup>10</sup> Based on our previous research on chiral primary amine catalysis, a cyclohexadiamine skeleton is selected as the primary aminocatalytic motif because of its simple structure and high reactivity as well as selectivity.<sup>7a–c,m</sup>

Supramolecular chiral diamine **CD-1** to **CD-6** were readily synthesized by nucleophilic substitution of mono-(*O*-6-tosyl)- $\beta$ -cyclodextrin with corresponding diamine in DMF at 80 °C under an argon atmosphere as previously described (Scheme 2).<sup>11</sup> After precipitation with a large quantity of acetone, pure products could be obtained in gram scale. Unlike native  $\beta$ -cyclodextrin, all the compounds are very soluble in water, which makes them suitable for catalytic applications in aqueous media.

Crystals of **CD-1** were obtained by slow evaporation of an aqueous solution at room temperature for a few weeks. X-ray crystallographic analysis proved the molecular structure of **CD-1** (Figure 1; see Supporting Information Table S4 for detailed crystal data). In the solid state, **CD-1** assembles into a linear

- (4) For asymmetric supramolecular catalysis with moderate enantioselectivity in aqueous media, see: ref 8g and (a) Fasella, E.; Dong, S. D.; Breslow, R. *Bioorg. Med. Chem.* **1999**, *7*, 709–714. (b) Rousseau, C.; Christensen, B.; Bols, M. *Eur. J. Org. Chem.* **2005**, 2734–2739. (c) Reddy, M. A.; Bhanumathi, N.; Rao, K. R. *Chem. Commun.* **2001**, 1974–1975. (d) Suresh, P.; Pitchumani, K. *Tetrahedron: Asymmetry* **2008**, *19*, 2037–2044. (e) Brown, C. J.; Bergman, R. G.; Raymond, K. N. *J. Am. Chem. Soc.* **2009**, *131*, 17530–17531. For examples of supramolecular photochirogenesis in aqueous media, see ref 17b, c and (f) Luo, L.; Liao, G.; Wu, X.; Lei, L.; Tung, C.-H.; Wu, L.-Z. *J. Org. Chem.* **2009**, *74*, 3506–3515. (g) Wada, T.; Nishijima, M.; Fujisawa, T.; Sugahara, N.; Mori, T.; Nakamura, A.; Inoue, Y. *J. Am. Chem. Soc.* **2003**, *125*, 7492–7493. (h) Nishijima, M.; Wada, T.; Mori, T.; Pace, T. C. S.; Bohne, C.; Inoue, Y. *J. Am. Chem. Soc.* **2007**, *129*, 3478–3479. (i) Nishijima, M.; Pace, T. C. S.; Nakamura, A.; Mori, T.; Wada, T.; Bohne, C.; Inoue, Y. *J. Org. Chem.* **2007**, *72*, 2707–2715. (j) Lu, R.; Yang, C.; Cao, Y.; Tong, L.; Jiao, W.; Wada, T.; Wang, Z.; Mori, T.; Inoue, Y. *J. Org. Chem.* **2008**, *73*, 7695–7701. (k) Nishioka, Y.; Yamaguchi, T.; Kawano, M.; Fujita, M. *J. Am. Chem. Soc.* **2008**, *130*, 8160–8161. (l) Yang, C.; Mori, T.; Inoue, Y. *J. Org. Chem.* **2008**, *73*, 5786–5794.
- (5) For a discussion, see: (a) Diederich, F. *Angew. Chem., Int. Ed.* **2007**, *46*, 68–69. For the reviews of construction for supramolecular cavity, see: (b) Hof, F.; Craig, S. L.; Nuckolls, C.; Rebek, J. J. *Angew. Chem., Int. Ed.* **2002**, *41*, 1488–1508. (c) Saalfrank, R. W.; Maid, H.; Scheurer, A. *Angew. Chem., Int. Ed.* **2008**, *47*, 8794–8824. (d) Kawase, T.; Kuruta, H. *Chem. Rev.* **2006**, *106*, 5250–5273. (e) Mateos-Timoneda, M. A.; Grego-Calama, M.; Reinhoudt, D. N. *Chem. Soc. Rev.* **2004**, *33*, 363–372.
- (6) (a) Mukherjee, S.; Yang, J. W.; Hoffman, S.; List, B. *Chem. Rev.* **2007**, *107*, 5471–5569. (b) Berkessel, A.; Groger, H. *Asymmetric Organocatalysis*; Wiley-VCH: Weinheim, 2005.
- (7) (a) Luo, S. Z.; Xu, H.; Li, J. Y.; Zhang, L.; Cheng, J.-P. *J. Am. Chem. Soc.* **2007**, *129*, 3074–3075. (b) Luo, S. Z.; Xu, H.; Chen, L.; Cheng, J.-P. *Org. Lett.* **2008**, *10*, 1775–1778. (c) Luo, S. Z.; Xu, H.; Zhang, L.; Li, J.; Cheng, J.-P. *Org. Lett.* **2008**, *10*, 653–656. (d) Xu, X.-Y.; Wang, Y.-Z.; Gong, L.-Z. *Org. Lett.* **2007**, *9*, 4247–4249. (e) Ramasastry, S. S. V.; Albertshofer, K.; Utsumi, N.; Tanaka, F.; Barbas, C. F., III. *Angew. Chem., Int. Ed.* **2007**, *46*, 5572–5575. (f) Li, J.; Luo, S. Z.; Cheng, J.-P. *J. Org. Chem.* **2009**, *74*, 1747–1750. (g) Ramasastry, S. S. V.; Zhang, H.; Tanaka, F.; Barbas, C. F., III. *J. Am. Chem. Soc.* **2009**, *129*, 288–289. (h) Utsumi, N.; Imai, M.; Tanaka, F.; Ramasastry, S. S. V.; Barbas, C. F., III. *Org. Lett.* **2007**, *9*, 3445–3448. (i) Ramasastry, S. S. V.; Albertshofer, K.; Utsumi, N.; Barbas, C. F., III. *Org. Lett.* **2008**, *10*, 1621–1624. (j) Zhu, M.-K.; Xu, X.-Y.; Gong, L.-Z. *Adv. Synth. Catal.* **2008**, *350*, 1390–1396. (k) Wu, X.; Ma, Z.; Ye, Z.; Qian, S.; Zhao, G. *Adv. Synth. Catal.* **2009**, *351*, 158–162. (l) Zheng, B.; Liu, Q.; Guo, C.; Wang, X.; He, L. *Org. Biomol. Chem.* **2007**, *5*, 2913–2915. (m) Luo, S. Z.; Qiao, Y.; Zhang, L.; Li, J.; Li, X.; Cheng, J.-P. *J. Org. Chem.* **2009**, *74*, 9521–9523.

- (8) For research on enzyme mimics based on cyclodextrin, see: (a) Breslow, R.; Dong, S. D. *Chem. Rev.* **1998**, *98*, 1997–2012. (b) Rekharsky, M. V.; Inoue, Y. *Chem. Rev.* **1998**, *98*, 1875–1918. (c) Iglesias, E. *J. Am. Chem. Soc.* **1998**, *120*, 13057–13069. (d) Ortega-Caballero, F.; Rousseau, C.; Christensen, B.; Petersen, T. E.; Bols, M. *J. Am. Chem. Soc.* **2005**, *127*, 3238–3239. (e) Ortega-Caballero, F.; Bjerre, J.; Laustsen, L. S.; Bols, M. *J. Org. Chem.* **2005**, *70*, 7217–7226. (f) Dong, Z.; Liu, J.; Mao, S.; Huang, X.; Yang, B.; Ren, X.; Luo, G.; Shen, J. *J. Am. Chem. Soc.* **2004**, *126*, 16395–16404. (g) Chan, W.-K.; Yu, W.-Y.; Che, C.-M.; Wong, M.-K. *J. Org. Chem.* **2003**, *68*, 6576–6582. (h) Yang, J.; Gabriele, B.; Belvedere, S.; Huang, Y.; Breslow, R. *J. Org. Chem.* **2002**, *67*, 5057–5067. (i) Rousseau, C.; Christensen, B.; Petersen, T. E.; Bols, M. *Org. Biomol. Chem.* **2004**, *2*, 3476–3482. (j) Báscuas, J.; García-Río, L.; Leis, J. R. *Org. Biomol. Chem.* **2004**, *2*, 1186–1193. (k) Chou, D. T. H.; Zhu, J.; Huang, X.; Bennet, A. J. *J. Chem. Soc., Perkin Trans. 2* **2001**, 83–89. (l) Iglesias, E.; Fernández, A. *J. Chem. Soc., Perkin Trans. 2* **1998**, 1691–1700. (m) Rousseau, C.; Ortega-Caballero, F.; Nordström, L. U.; Christensen, B.; Petersen, T. E.; Bols, M. *Chem.—Eur. J.* **2005**, *11*, 5094–5101. (n) Bjerre, J.; Nielsen, E. H.; Bols, M. *Eur. J. Org. Chem.* **2008**, 745–752. (o) Marinescu, L. G.; Bols, M. *Angew. Chem., Int. Ed.* **2006**, *45*, 4590–4593.
- (9) (a) Breslow, R.; Graff, A. *J. Am. Chem. Soc.* **1993**, *115*, 10988–10989. (b) Desper, J. M.; Breslow, R. *J. Am. Chem. Soc.* **1994**, *116*, 12081–12082. (c) Yuan, D.-Q.; Dong, S. D.; Breslow, R. *Tetrahedron Lett.* **1998**, *39*, 7673–7676. (d) Tagaki, W.; Yamamoto, H. *Tetrahedron Lett.* **1991**, *32*, 1207–1208. (e) Yuan, D.-Q.; Xie, R. G.; Zhao, H. M. *Chin. Chem. Lett.* **1991**, *2*, 617–620. (f) Watanabe, K.; Yamada, Y.; Goto, K. *Bull. Chem. Soc. Jpn.* **1985**, *58*, 1401–1406.
- (10) (a) Liu, K.; Haussinger, D.; Woggon, W. D. *Synlett* **2007**, 2298–2300. (b) Shen, Z. X.; Ma, J. M.; Liu, Y. H.; Jiao, C. J.; Li, M.; Zhang, Y. W. *Chirality* **2005**, *17*, 556–558. (c) Huang, J.; Zhang, X.; Armstrong, D. W. *Angew. Chem., Int. Ed.* **2007**, *46*, 9073–9077.
- (11) Petter, R. C.; Salek, J. S.; Sikorski, C. T.; Kumaravel, G.; Lin, F. T. *J. Am. Chem. Soc.* **1990**, *112*, 3860–3868.

Scheme 2<sup>a</sup>

<sup>a</sup> (a) Representative synthetic route for supramolecular diamine catalyst. (b) Supramolecular diamine catalysts **CD-1** to **CD-6** and small molecular analogues **7** to **10**.

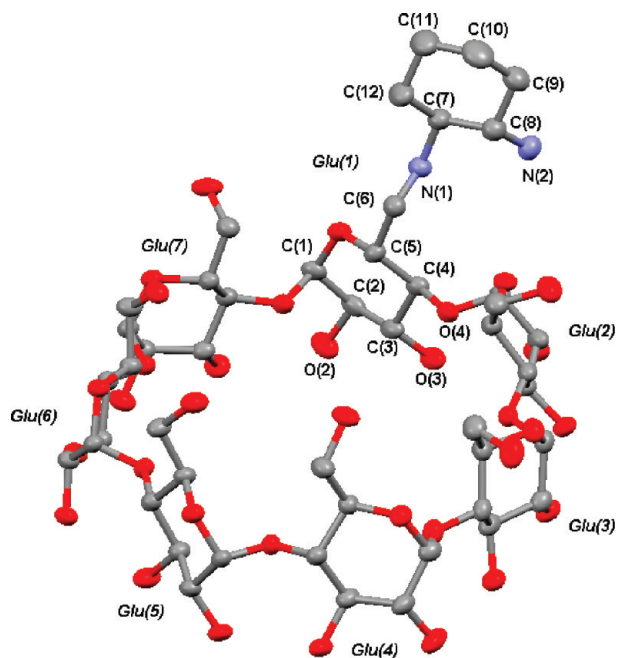


Figure 1. Crystal structure of **CD-1**.

columnar suprastructure, wherein the appended cyclohexadiamine group is intermolecularly encapsulated in the hydrophobic cavity of an adjacent cyclodextrin *via* the secondary rim (Figure 2). Similar assembly structures have also been observed in several other 6-substituted  $\beta$ -cyclodextrins.<sup>12</sup> Consistent with previous reports, the hydrogen bonding together with hydrophobic interactions stabilizes the intermolecular self-assembly and columnar structure in the crystalline state.

**2. Direct Aldol Reaction Catalyzed by Cyclodextrin Derivatives.** With chiral supramolecular primary amine catalysts in hand, we proceeded to test their catalytic ability in asymmetric

direct aldol reactions. Previously, significant efforts have been made to mimic the aldolase I mediated processes using a supramolecular system. Unfortunately, no enantioselectivity has been achieved in these studies.<sup>9</sup> Even in the golden age of organocatalysis, where small molecules like L-proline have been shown to mimic mechanistically aldolase I with spectacular stereocontrol, the realization of such catalysis under enzymatic conditions, i.e. buffered aqueous media with reasonable enantioselectivity, remains an elusive goal.<sup>13</sup> In this context, it is delightful to find that the primary-secondary diamine catalyst **CD-1** is indeed a viable aldol catalyst in an aqueous buffer solution with good enantioselectivity. Using the reaction of acetone and *p*-nitrobenzaldehyde as a model reaction, the pH–activity/stereoselectivity profiles of **CD-1** were determined (Figure 3), and the optimal pH was found to be approximately

- (12) (a) Liu, Y.; You, C.-C.; Zhang, M.; Weng, L.-H.; Wada, T.; Inoue, Y. *Org. Lett.* **2000**, 2, 2761–2763. (b) Hirotsu, K.; Higuchi, T.; Fujita, K.; Ueda, T.; Shinoda, A.; Imoto, T.; Tabushi, I. *J. Org. Chem.* **1982**, 47, 1143–1144. (c) Kamitori, S.; Hirotsu, K.; Higuchi, T.; Fujita, K.; Yamamura, H.; Imoto, T.; Tabushi, I. *J. Chem. Soc., Perkin Trans. 2* **1987**, 7–14. (d) Harata, K.; Rao, C. T.; Pitha, J. *Carbohydr. Res.* **1993**, 247, 83–98. (e) Mentzafos, D.; Terzis, A.; Coleman, A. W.; de Rango, C. *Carbohydr. Res.* **1996**, 282, 125–135. (f) Yoshida, N.; Harata, K.; Inoue, T.; Ito, N.; Ichikawa, K. *Supramol. Chem.* **1998**, 10, 63–67.
- (13) For discussions and reviews on aqueous organocatalysis, see: (a) Brogan, A. P.; Dickerson, T. J.; Janda, K. D. *Angew. Chem., Int. Ed.* **2006**, 45, 8100–8102. (b) Hayashi, Y. *Angew. Chem., Int. Ed.* **2006**, 45, 8103–8104. (c) Blackmond, D. G.; Armstrong, A.; Coombe, V.; Wells, A. *Angew. Chem., Int. Ed.* **2007**, 46, 3798–3800. (d) Narayan, S.; Muldoon, J.; Finn, M. G.; Fokin, W.; Kolb, H. C.; Sharpless, K. B. *Angew. Chem., Int. Ed.* **2005**, 44, 3275–3279. (e) Mlynarski, J.; Paradowska, J. *Chem. Soc. Rev.* **2008**, 37, 1502–1511. (f) Paradowska, J.; Stodulski, M.; Mlynarski, J. *Angew. Chem., Int. Ed.* **2009**, 48, 4288–4297. For several examples of aldol reaction catalyzed in buffer, see: (g) Reymond, J. L.; Chen, Y. *J. Org. Chem.* **1995**, 60, 6970–6979. (h) Dickerson, T. J.; Janda, K. D. *J. Am. Chem. Soc.* **2002**, 124, 3220–3221. (i) Córdova, A.; Notz, W.; Barbas, C. F., III. *Chem. Commun.* **2002**, 3024–3025. (j) Li, J.; Hu, S.; Luo, S. Z.; Cheng, J.-P. *Eur. J. Org. Chem.* **2009**, 132–140.



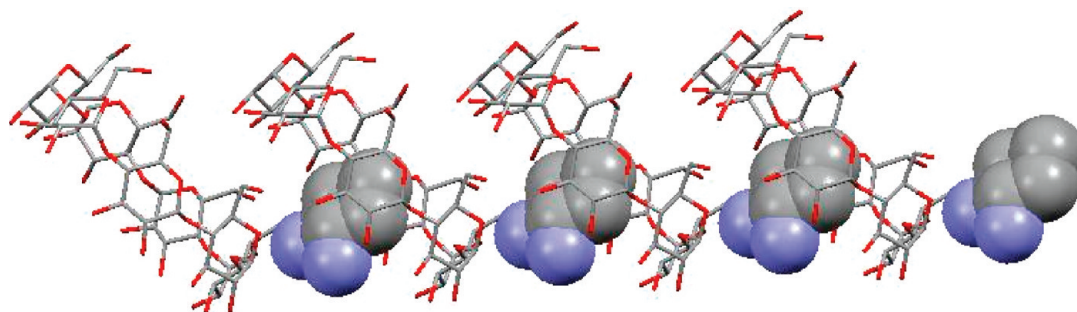


**Figure 2.** Side view of the crystal packing in solid state along  $\alpha$ -axis.

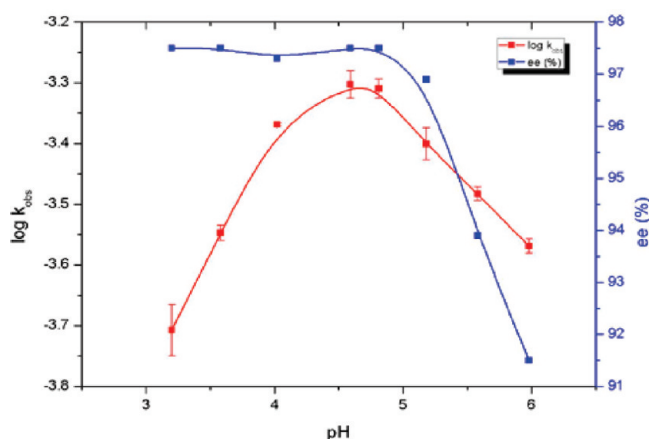


**Figure 3.** Correlation of pH value with  $\log k_{\text{obs}}$  and  $ee$  of the model reaction catalyzed by **CD-1** at 25 °C in 50 mM acetate buffer (1.0 mL) containing **CD-1** (0.2 mM), *p*-nitrobenzaldehyde (4 mM), acetone 5% (v/v).

4.60–4.80 in terms of both activity and enantioselectivity.<sup>14</sup> It is noteworthy that no apparent dehydration and retro-aldol products were observed under such conditions and the desired aldol product was obtained with excellent enantioselectivity (97%  $ee$ ), representing the best results that could be achieved in pure buffered aqueous media for this reaction.

The kinetics of the catalytic reaction by **CD-1** in aqueous acetate buffer was investigated next. The reaction was found to follow Michaelis–Menten kinetics at pH 4.80 and 25 °C in the presence of excess acetone (5% v/v), showing a Lineweaver–Burk plot with a  $K_m = 6.31$  mM and a  $k_{\text{cat}} = 6.07 \times 10^{-3} \text{ min}^{-1}$  (Figure 4). To understand the nature of the catalysis, the cyclodextrin analogues **CD-2** to **CD-6** and organocatalysts **7** to **10** were then examined in the model reaction (Table 1). Though the small molecular catalysts such as primary-tertiary diamine **7** and primary-secondary diamine **8** were able to promote the model reactions as well in aqueous buffer, the reactions generally showed low activity and poor stereoselectivity (Table 1, entries 7–9). No further improvements were observed when the small molecular diamines are endowed with long alkyl chains such as in diamines **9** and **10** (Table 1, entry 10, 11) or with the use of  $\beta$ -cyclodextrin as an additive (Table 1, entry 12). In sharp contrast, covalently connecting a primary-secondary diamine (e.g., ent-**8**) with  $\beta$ -cyclodextrin (i.e., **CD-1**) led to a dramatically improved enantioselectivity and an over 6-fold rate acceleration compared with the parent ent-**8** (Table 1, entry 1 vs 9). Note also that the stereoselectivity was switched

from *S* in catalysis with ent-**8** to *R* with supramolecular **CD-1**. Remarkably, the *R* selectivity was maintained in catalysis with **CD-1**–**CD-4**, regardless of the configurations of the appended diamines. These results suggest that the cyclodextrin cavity plays a decisive role in controlling stereoselectivity. In addition, the catalysis of **CD-1** could be inhibited by the addition of 1-bromoadamantane, a known good guest for  $\beta$ -cyclodextrin (Table 1, entry 13), further confirming that the cyclodextrin cavity must have been involved in the catalytic coordinate.

It is observed that **CD-1**, which differs with **CD-2** only on the absolute configuration of the appended cyclohexanediamine, demonstrated superior catalytic efficacy (Table 1, entry 1 vs 2, 3 times faster) and enantioselectivity (97%  $ee$  vs 68%  $ee$ ). These results together with the inefficiency of *cis*-cyclohexanediamine-appended **CD-3** suggest the match and mismatch of configurations in this series of catalysts. In addition, the observation that catalysts containing tertiary amine or secondary amine such as **CD-5** and **CD-6** were totally inert in aqueous buffer further proves the advantage of bifunctional primary amine catalysis in **CD-1**.

**3. Substrate Scope.** The catalysis of **CD-1** and **CD-2** was next examined with a variety of substrates. The results are presented in Table 2 where some characteristics of the supramolecular catalysis are evident. (1) The reactions not only tolerate a range of aromatic aldehydes but also demonstrate interesting features on recognition over different acceptors. For example, while the reaction of 2-naphthaldehyde proceeded smoothly, 1-naphthaldehyde resulted in being a quite sluggish substrate (Table 2, entry 6 vs 5), suggesting that the proper geometry and orientation of an acceptor in the cyclodextrin cavity are required for effective catalysis. (2) The catalysis is highly size sensitive for aldol donors, and among a range of ketone donors examined, only the small donors such as acetone, butanone, and cyclopentanone are identified to be effective substrates for **CD-1**. Note that the reaction of cyclohexanone is more than 46 times slower than that of cyclopentanone caused by just one more  $\text{CH}_2$  unit (Table 2, entry 11 vs 13). Interestingly, the diastereoselectivity in the reaction of cyclopentanone is switched from *anti* to *syn* by using **CD-2** instead of **CD-1**, whereas the same level of enantioselectivity is maintained for the major isomer (Table 2, entry 11 vs 12). (3) The catalysis of **CD-1** could be applied under high concentration (up to 0.25 M) while maintaining similar activity and enantioselectivity (Table 2, entries 1, 2, 6, 10–12; see Supporting Information Table S2 for details). These features indicate an effective supramolecular approach to asymmetric organocatalysis that works smoothly in aqueous buffer with synthetic practicality.<sup>13g–j</sup> Under the latter conditions, the reaction appears to be heterogeneous and thus vigorous stirring should be applied to facilitate a smooth reaction.

(14) At pH > 6.0, the reaction rate increases but with significantly reduced enantioselectivity, indicating the existence of a general base catalyzed by-pathway under this condition.

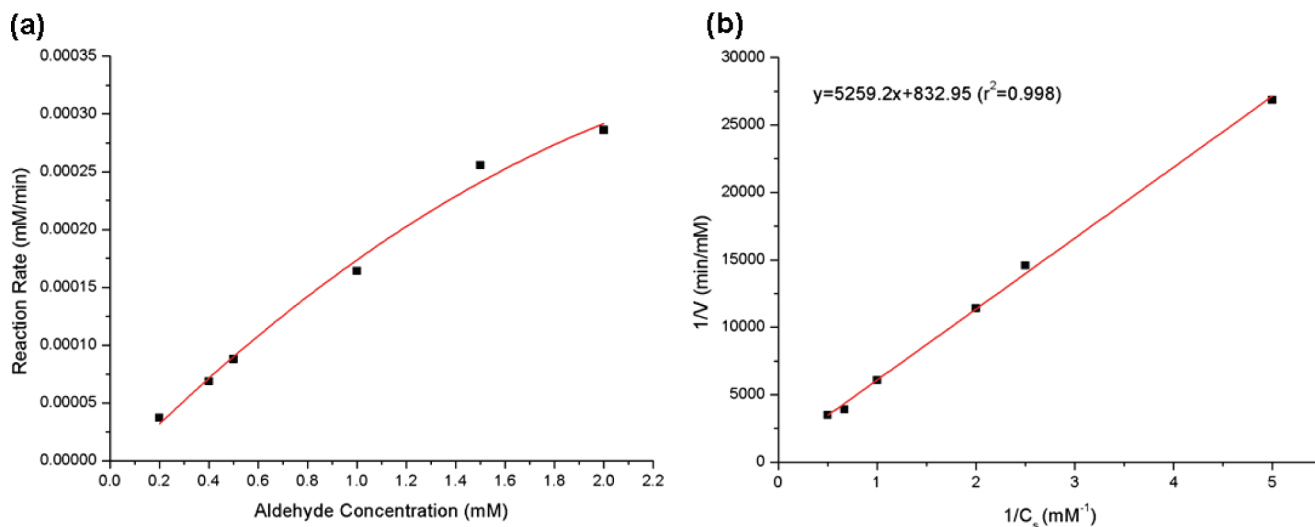


**Figure 4.** (a) Michaelis–Menten curves and (b) Lineweaver–Burk plot for **CD-1** catalyzed model reaction at 25 °C in 50 mM acetate buffer (pH = 4.80, 1.0 mL) containing **CD-1** 0.2 mM, acetone 5% (v/v).

**Table 1.** Asymmetric Supramolecular Catalysis of Direct Aldol Reaction<sup>a</sup>

Entry	Cat.	$k_{rel}$	$ee$ (%)	
1	<b>CD-1</b>	6.45	97 ( <i>R</i> )	
2	<b>CD-2</b>	2.06	68 ( <i>R</i> )	
3	<b>CD-3</b>	0.22	54 ( <i>R</i> )	
4	<b>CD-4</b>	0.68	22 ( <i>R</i> )	
5	<b>CD-5</b>	0.054	n.d. <sup>e</sup>	
6	<b>CD-6</b>	0.038	n.d. <sup>e</sup>	
7	<b>7</b>	0.66	9 ( <i>S</i> )	
8	<b>8</b>	1.00	20 ( <i>R</i> )	
9	<b>Ent-8</b>	1.00	20 ( <i>S</i> )	
10	<b>9</b>	0.20	13 ( <i>S</i> )	
11	<b>10</b>	1.23	31 ( <i>R</i> )	
12 <sup>b</sup>	<b>8</b>	1.03	20 ( <i>R</i> )	
13 <sup>c</sup>	<b>CD-1</b>	0.76	63 ( <i>R</i> ) <sup>d</sup>	

<sup>a</sup> Conditions: catalyst 0.2 mM, acetone 5% (v/v), aldehyde 4 mM, 25 °C, 50 mM acetate buffer (pH = 4.80, 1 mL). <sup>b</sup>  $\beta$ -Cyclodextrin (0.2 mM) was added. <sup>c</sup> 1-Bromoadmantane (8 mM) was added as inhibitor. <sup>d</sup> Dehydration product was observed. <sup>e</sup> The  $ee$  of the product is not determined.

**4. Mechanism Studies.** Detailed mechanism studies were carried out next to gain more insights into this intriguing asymmetric supramolecular catalysis. Accordingly, typical techniques and methods in both supramolecular recognition studies and in catalytic mechanism studies were utilized in concert to explore the recognition properties, conformational changes, and the possible catalytic cycles. **CD-1**, **CD-2**, and (1-, and 2-) naphthaldehydes were selected as the representative catalysts and substrates, respectively. When necessary, some other tested substrates as shown in Table 2 were also included in the study for comparison.

**4.1. Recognition Behaviors of CD-1 and CD-2 toward Substrates.** The molecular recognition between catalyst and aldol acceptor naphthaldehydes was probed with the aid of fluorescence and circular dichroism spectroscopy in acetate buffer (pH = 4.80). A series of naphthalene derivatives such as naphthalenylmethanol, naphthol, and naphthanoic acid were also incorporated in this study. Pronounced fluorescence changes

**Table 2.** Asymmetric Supramolecular Catalysis of Direct Aldol Reaction<sup>a</sup>

Entry	R	R¹	Cat.	$k_{obs}$ <sup>b</sup>	$ee$ (%)	$dr$ <sup>d</sup>	
1	H	4-NO <sub>2</sub> Ph	<b>CD-1</b>	94.2 (91) <sup>c</sup>	97	---	
2	H	Ph	<b>CD-1</b>	10.9 (67) <sup>c</sup>	91	---	
3	H	4-MePh	<b>CD-1</b>	13.2	92	---	
4	H	4-MeOPh	<b>CD-1</b>	4.01	93	---	
5	H	1-Naphth	<b>CD-1</b>	0.62	71	---	
6	H	2-Naphth	<b>CD-1</b>	32.5 (61) <sup>c</sup>	97	---	
7	H	4-PhPh	<b>CD-1</b>	12.1	>99	---	
8	H	piperonal	<b>CD-1</b>	4.02	94	---	
9	H	2-Naphth	<b>CD-2</b>	4.39	90	---	
10	H, Me	4-NO <sub>2</sub> Ph	<b>CD-1</b>	35.6 (75) <sup>c</sup>	90/99	53/47	
11	-(CH <sub>2</sub> ) <sub>2</sub> -	4-NO <sub>2</sub> Ph	<b>CD-1</b>	558 (98) <sup>c</sup>	48/82	25/75	
12	-(CH <sub>2</sub> ) <sub>2</sub> -	4-NO <sub>2</sub> Ph	<b>CD-2</b>	262 (94) <sup>c</sup>	81/55	65/34	
13	-(CH <sub>2</sub> ) <sub>3</sub> -	4-NO <sub>2</sub> Ph	<b>CD-1</b>	12.0	23/96	14/86	

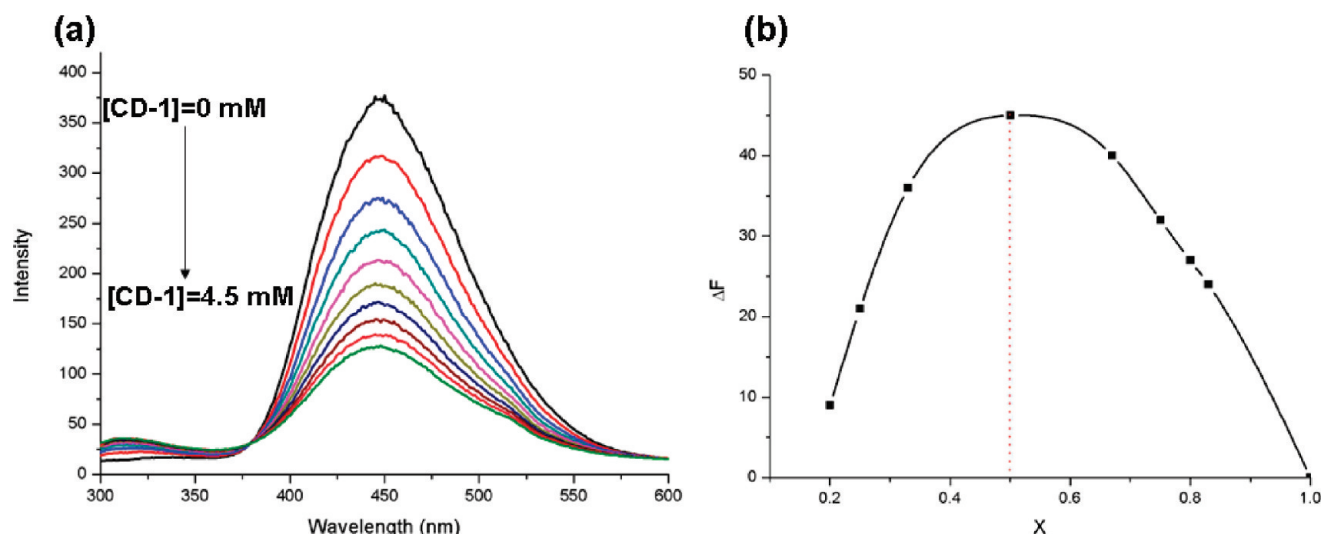
<sup>a</sup> Conditions: catalyst 0.2 mM, aldehyde 4 mM, 25 °C, 50 mM acetate buffer (pH = 4.80, 1 mL), donor 10% (v/v). <sup>b</sup> Expressed in unit of 10<sup>-5</sup> mM/min. <sup>c</sup> Percent yield with 250 mM aldehyde in 12–48 h. <sup>d</sup> *Syn/anti* determined by HPLC or <sup>1</sup>H NMR.

were observed when naphthaldehyde was treated with a solution of CD catalyst. For example, fluorescence intensity was decreased when **CD-1** was added to a dilute solution of 2-naphthaldehyde solution in acetate buffer (Figure 5a). A Job plot<sup>15</sup> showed that 2-naphthaldehyde and **CD-1** formed a 1:1 complex in an acetate buffer solution (Figure 5b).

The association constants of **G1** to **G9** with native  $\beta$ -CD and our CD catalysts were then determined using fluorescence spectroscopy, and the obtained association constants are summarized in Table 3.<sup>16</sup> Several binding features can be summarized based on the data in Table 3: (1) The binding affinities of **CD-1** and **CD-2** toward naphthaldehyde analogues such as naphthenylmethanol **G1** and naphthol **G2** are generally decreased compared to those with native  $\beta$ -CD (Table 3, entries

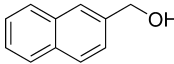
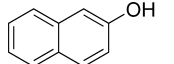
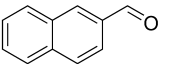
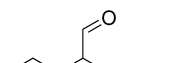
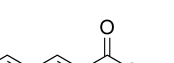
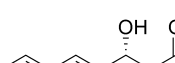
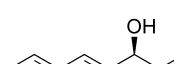
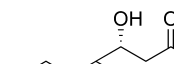

(15) Job, P. *Ann. Chim.* **1928**, 9, 113–203.

(16) The measurement of binding constants follows the method presented in Connor, K. A. *Binding Constants: The measurement of Molecular Complex Stability*; John Wiley & Sons: New York, 1987.



**Figure 5.** (a) The family of fluorescence spectra of 0.02 mM of 2-naphthaldehyde aqueous solution at various concentrations of **CD-1** (0 to 4.5 mM). (b) The job's plot of change in the fluorescence spectrum. [2-Naphthaldehyde] + [CD-1] = 0.24 mM.

**Table 3.** Association Constants ( $K_a$ ) for the Complexation of **G1** to **G9** with Cyclodextrin Catalyst<sup>a</sup>

		
<b>G1</b>	<b>G2</b>	<b>G3</b>
		
<b>G4</b>	<b>G5</b>	<b>G6</b>
		
<b>G7</b>	<b>G8</b>	<b>G9</b>

Entry	Host	Guest	$K_a$ (L · mol <sup>-1</sup> )
1	CD-1	G1	45
2	CD-2	G1	36
3	$\beta$ -CD	G1	389
4	CD-1	G2	148
5	CD-2	G2	182
6	$\beta$ -CD	G2	395
7	CD-1	G3	403
8	CD-2	G3	339
9	$\beta$ -CD	G3	226
10	CD-1	G4	60
11	CD-2	G4	n.d. <sup>b</sup>
12	$\beta$ -CD	G4	n.d. <sup>b</sup>
13	CD-1	G5	1057
14	CD-2	G5	741
15	$\beta$ -CD	G5	198
16	CD-1	G6	200
17	CD-1	G7	212
18	CD-1	G8	218
19	CD-1	G9	215

<sup>a</sup> Solvent: 50 mM acetate buffer (pH = 4.80) containing 2% glycol.

<sup>b</sup> The binding affinities are bellowing the measurement limits of fluorescence titration. See Figure S3a in the Supporting Information for the representative fluorescence spectra under this situation.

1, 2 vs 3, entries 4, 5 vs 6), suggesting some interferences of the appended cyclohexadiamine moiety to binding in these cases. Remarkably, (2) this interference is reversed to favorable binding

when the hydroxymethylene group is changed to formyl (the substrate in our catalysis) and carboxyl groups as in the cases of **G3** and **G5** (Table 3, entries 7, 8, 13, 14). Compared to native β-CD, the bindings of both **CD-1** and **CD-2** toward these guests are significantly enhanced. Clearly, additional interactions between the diamino group side chain and carbonyl group of substrates, e.g. hydrogen bonding, electrostatic interactions, or even covalent Schiff base formation, should contribute modestly to the binding besides the hydrophobic effect. A similar effect has also been observed in other amino-substituted cyclodextrins when binding with carbonyl compounds.<sup>17</sup> Regarding the structural impact on binding, (3) it is noted that a stronger binding affinity is generally observed with **CD-1** than that with **CD-2** in recognizing **G3** to **G4**, (4) whereas 2-substituted naphthalenes are much better guest molecules than 1-substituted naphthalenes for both **CD-1** and **CD-2**. In both cases, the observed binding phenomena are consistent with the respective catalytic behaviors, serving as a reminder that stronger substrate binding leads to better catalytic outcome. For example, with a modest enhancement of binding with **CD-1** over **CD-2** (Table 3, entry 7 vs 8,  $K_a = 403 \text{ L} \cdot \text{mol}^{-1}$  vs  $339 \text{ L} \cdot \text{mol}^{-1}$ ), the reaction of 2-naphthaldehyde (**G3**) catalyzed by **CD-1** is 7 times faster than that catalyzed by **CD-2** (Table 2, entry 6 vs 9). In another example, **CD-1** binds 2-naphthaldehyde 7 times stronger than 1-naphthaldehyde (Table 3, entry 7 vs 10), corresponding to an over 50-fold rate increase and a significant improvement of *ee* (27%) for the reaction of the former over the latter (Table 2, entry 6 vs 5).

The association constants between **CD-1** and each of the enantiomers of aldol products (**G6–G9**) were also determined (Table 3, entries 16–19).<sup>18</sup> Interestingly, **CD-1** demonstrates a nearly identical binding affinity with association constants  $K_a \approx 200 \text{ L} \cdot \text{mol}^{-1}$  for all the four tested aldol products regardless of their absolute configurations, indicating chiral recognition is not occurring in our catalytic system. In addition, the lower binding affinity of product (**G6**) than substrate (**G3**) suggests that product inhibition would not happen under this context,

(17) (a) Kean, S. D.; May, B. L.; Clements, P.; Lincoln, S. F.; Easton, C. J. *J. Chem. Soc., Perkin Trans. 2* **1999**, 1257–1264. (b) Nakamura, A.; Inoue, Y. *J. Am. Chem. Soc.* **2005**, 127, 5338–5339. (c) Ke, C.; Yang, C.; Mori, T.; Wada, T.; Liu, Y.; Inoue, Y. *Angew. Chem., Int. Ed.* **2009**, 48, 6675–6677.



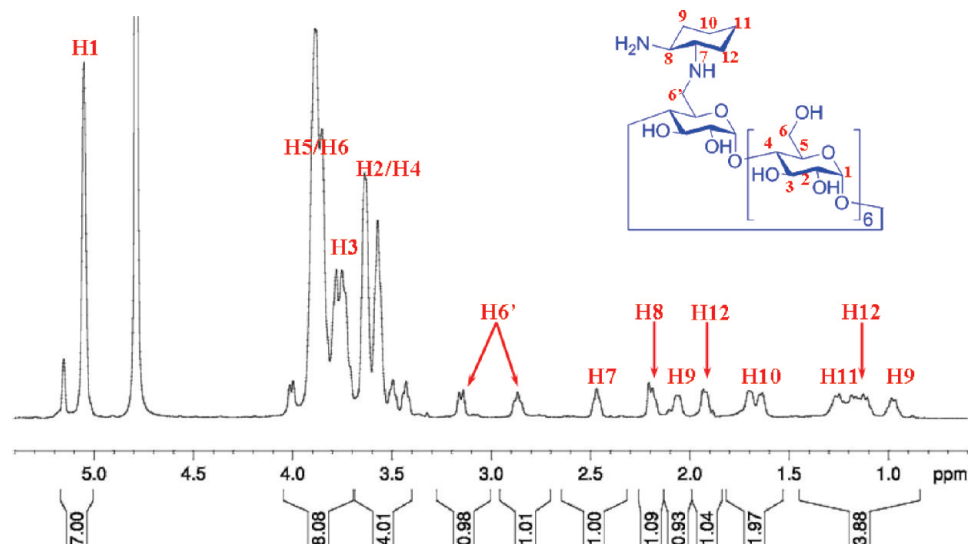


Figure 6. Assignment of  $^1\text{H}$  NMR of **CD-1**.

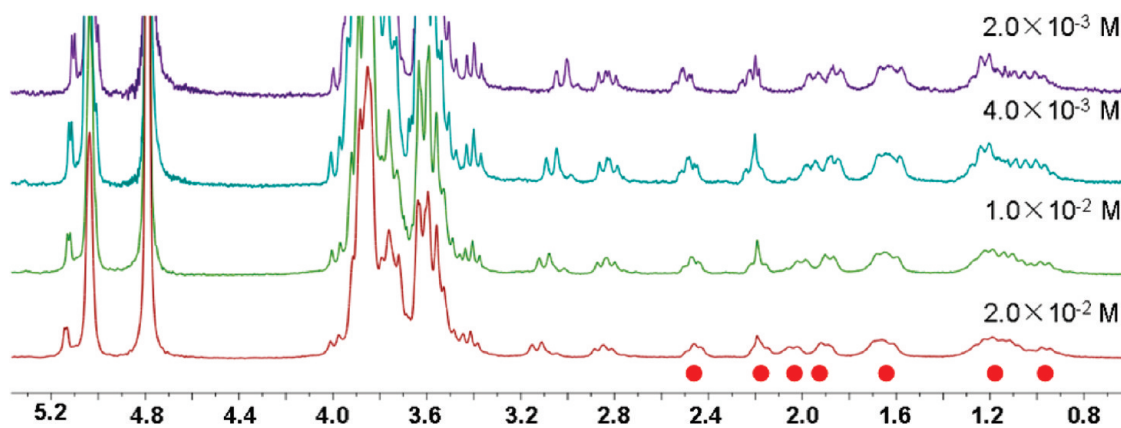


Figure 7.  $^1\text{H}$  NMR spectra of **CD-1** in  $\text{D}_2\text{O}$  with different concentrations. The red dot denotes the protons on cyclohexyl ring.

which may serve as the basis for catalytic turnovers in this chiral supramolecular system.

**4.2. Conformational Analysis of CD Catalysts in Solution and upon Binding with Substrates.** **4.2.1. Conformation of **CD-1** and **CD-2** in Water and Acetate Buffer (pH 4.8).** Unlike their solid intermolecularly self-assembled structures, 6-monosubstituted  $\beta$ -CD derivatives, particularly those with hydrophobic 6-substitutes, tend to form self-included structures in solution phase as demonstrated by numerous previous studies.<sup>19</sup> In our case, the conformation of **CD-1** in water was first analyzed using 1D and 2D NMR spectroscopy. The  $^1\text{H}$  signals of **CD-1** and **CD-2** in  $\text{D}_2\text{O}$  and acetate buffer (pH = 4.80) were fully assigned by the assistance of COSY, TOCSY, and HSQC spectrum (Figure 6; for details see Figures S7, S8 in the Supporting Information). No significant variations (<0.1 ppm) were ob-

served in the  $^1\text{H}$  NMR spectra of **CD-1**, particularly regarding the proton signals on the cyclohexyl ring under different concentrations (Figure 7). The DOSY spectrum of **CD-1** under 2 mM and 20 mM indicated the existence of a dominant single solution species with a similar diffusion coefficient under both low and high concentration (see Figure S10 in the Supporting Information), suggesting intermolecular assembly is not occurring under high concentration. All together, these observations rule out the possible intermolecular assembly of **CD-1** in solution. Therefore, **CD-1** would mainly exist as self-included conformations in pure water solution, which is consistent with previous conformational studies on similar 6-substituted cyclodextrins.<sup>19d,20</sup> An ROESY spectrum of **CD-1** provides further support to this conclusion (Figure 8; for the full ROESY spectrum see Figure S9 in the Supporting Information). As shown in Figure 8a, all the protons of the cyclohexyl ring correlate strongly with H5, the inner protons near the primary rim of the cyclodextrin cavity, while the correlations with H3, the inner protons near the secondary rim of cyclodextrin, are relatively weak, illustrating the formation of intramolecular self-assembly as depicted in the inside diagram (Figure 8a).

(18) The **CD-1**–product complexes exhibit distinctive fluorescence behavior (Figure S3b), indicating quite complicated binding processes beyond simple 1:1 host–guest interactions like those in **CD-1**–substrate systems. Apparent association constants (as listed in Table 3) were determined based on the fluorescence change.

(19) (a) Park, K. K.; Kim, Y. S.; Lee, S. Y.; Song, H. E.; Park, J. W. *J. Chem. Soc., Perkin Trans. 2* **2001**, 2, 2114–2113. (b) Liu, Y.; You, C.-C.; Kunieda, M.; Nakamura, A.; Wada, T.; Inoue, Y. *Supramol. Chem.* **2000**, 12, 299–316. (c) Li, D.; Ng, S.-C.; Novak, I. *Tetrahedron Lett.* **2002**, 43, 1871–1875. (d) Park, J. W.; Lee, S. Y.; Song, H. J.; Park, K. K. *J. Org. Chem.* **2005**, 70, 9505–9513.

(20) McAlpine, S. R.; Garcia-Garibay, M. A. *J. Am. Chem. Soc.* **1998**, 120, 4269–4275.

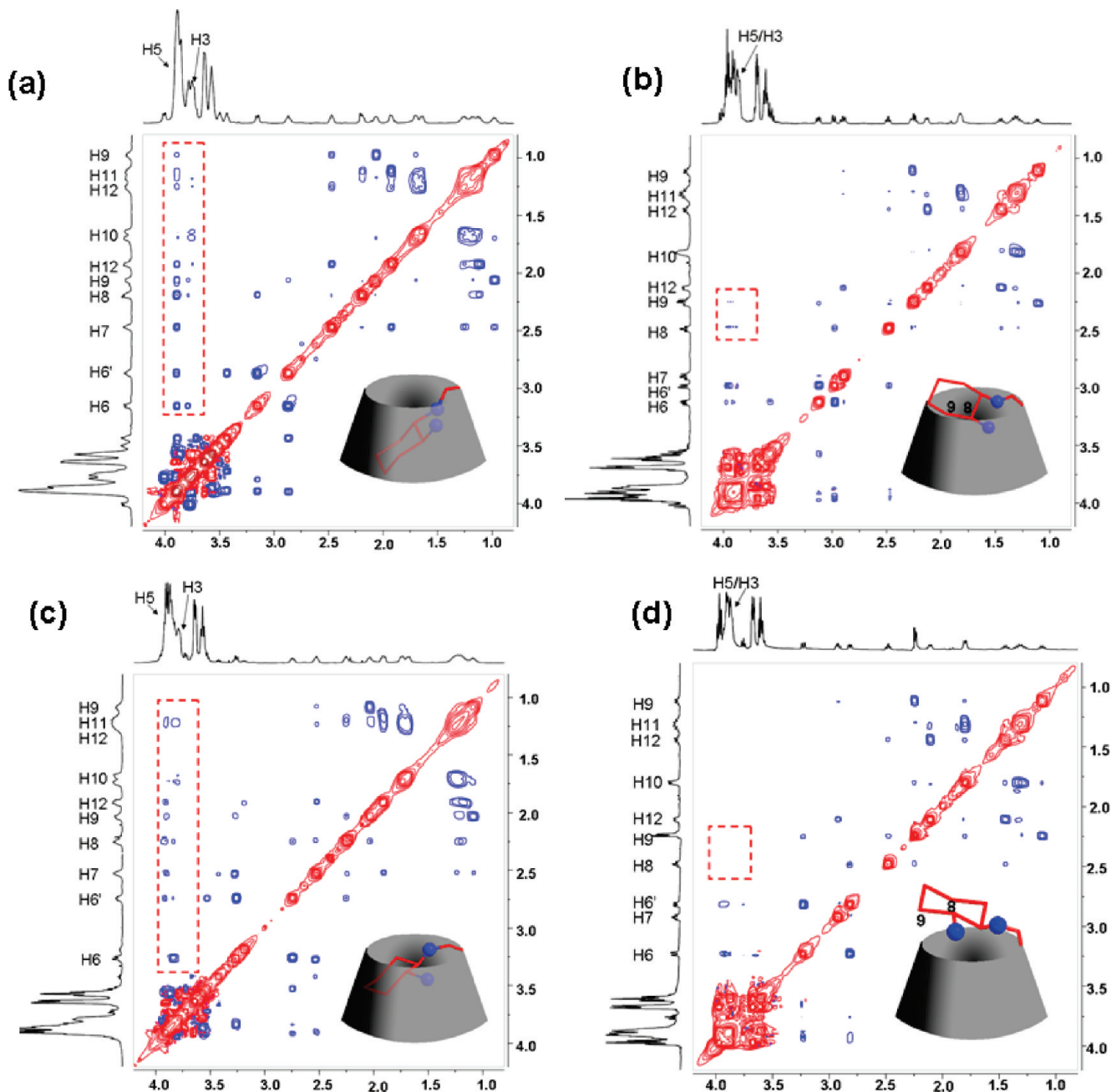


**Figure 8.** ROESY spectrum and conformation of (a) **CD-1** (0.02 M) in  $D_2O$ ; (b) **CD-1** (0.02 M) in acetate buffer (pH = 4.80); (c) **CD-2** (0.02 M) in  $D_2O$ ; and (d) **CD-2** (0.02 M) in acetate buffer (pH = 4.80).

Under catalytic conditions, i.e. acetate buffer (pH = 4.80), **CD-1** would become protonated with an estimated  $pK_a$  (**CD-1-H<sub>2</sub><sup>+</sup>**) of  $\sim 5.70$ .<sup>21</sup> As a result, H7–H12 signals on the protonated (*S,S*)-cyclohexadimine ring would be shifted lower compared with the neutral **CD-1**. In addition, the protonation of cyclohexadimine would decrease its hydrophobicity and thus cause exclusion of the suspended side chain from the cyclodextrin cavity,<sup>17a</sup> leading to protons being shifted even lower as shown in Figure 9. Indeed, the ROESY spectrum of **CD-1** in acetate buffer shows only weak correlations between H8, H9, and H5, a clear indication of the shallowly included (*S,S*)-cyclohexadimine group (Figure 8b).

The solution phase conformation of **CD-2**, which differs from **CD-1** in the absolute configuration of suspended cyclohexadimine, has also been studied. The ROESY spectrum indicates a similar conformation change as in the case of **CD-1** in which the suspended (*R,R*)-cyclohexadimine of **CD-2** is self-included in the cavity in pure water solution but excluded from the cavity in acidic acetate buffer (Figure 8c and 8d). Close analysis of the ROESY spectrum of both **CD-1** and **CD-2** in acidic acetate buffer reveals some delicate but noticeable differences. For comparison, the correlation signals of H12<sup>a</sup>–H12<sup>e</sup> are selected as references for the evaluation of relative intensities of cross peaks, as these self-correlations of H12 protons would be much less influenced by side chain configurations of **CD-1** and **CD-2** and are also relatively condition-independent.<sup>22</sup> Accordingly, there are much stronger correlations between H5, H8, and H9

(21) The  $pK_a$  (**CD-1-H<sub>2</sub><sup>+</sup>**) was estimated to be  $\sim 5.70$  according to May, B. L.; Kean, S. D.; Easton, C. J.; Lincoln, S. F. *J. Chem. Soc., Perkin Trans. 1* **1997**, 3157–3160.



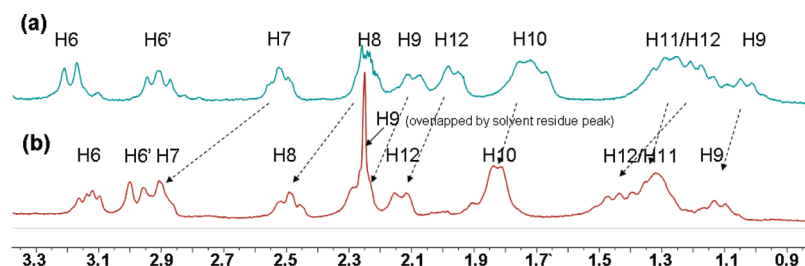


**Figure 9.**  $^1\text{H}$  NMR spectra of (a) **CD-1** (0.02 M) in  $\text{D}_2\text{O}$  and (b) **CD-1** (0.02 M) in acetate buffer ( $\text{pH} = 4.80$ ).

in **CD-1** than those in **CD-2** under acidic acetate conditions (see the area with red square in Figure 8b and 8d).<sup>22</sup> These observations are consistent with the model that the side chain of **CD-1** is shallowly included in the CD cavity, whereas the side chain of **CD-2** is likely suspended from the cavity. A preliminary molecular modeling study also verifies this conclusion.<sup>23</sup> This model well rationalizes the observations that **CD-2** exhibits a relatively poorer binding affinity toward guest **G3** and **G5** than **CD-1** (Table 3, entry 8 vs 7, entry 14 vs 13) since the possible noncovalent interactions between the suspended diamino moiety and the encapsulated guest, which would contribute in the binding, are geometrically less favorable in this context. Previously, an absolute configuration difference of side chains has been reported to cause a different self-inclusion depth, which consequently leads to different binding properties.<sup>24</sup>

**4.2.2. Substrate Binding Mode and Conformation Change of CD-1 upon Binding.** The substrate binding mode of our optimal catalyst **CD-1** as well as the accompanying conformational changes was next probed. The hydrophobic interactions provided by the cavity of cyclodextrin are the major driving forces for the formation of a catalyst–substrate complex in aqueous media, which has been extensively researched in the supramolecular system.<sup>25</sup> Moreover, the cavity of cyclodextrin has a certain degree of rigidity because of the hydrogen-bonding network among the hydroxyl groups on the rims. Thus, the match in sizes between guests and hosts is also of great importance in the course of recognition. With these factors noted, some initial knowledge regarding the binding mode of **CD-1** is easily conceivable. For example, according to Harata's previous study,<sup>26</sup> 2-substituted naphthalene forms an axial inclusion in the cyclodextrin cavity while 1-substituted naphthalene tends to form equatorial inclusion.<sup>26a,27</sup> Therefore, in

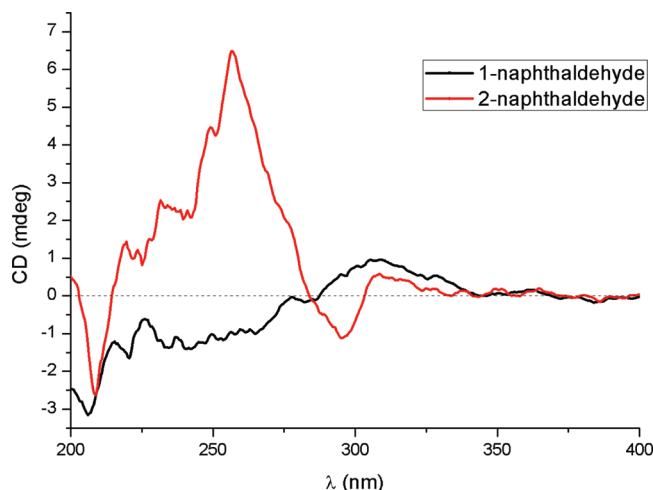


**Figure 10.** Circular dichroism spectrum of 1-naphthaldehyde (0.04 mM, black line) and 2-naphthaldehyde (0.04 mM, red line) in 50 mM acetate buffer ( $\text{pH} = 4.80$ ) containing 10% acetonitrile and 2.0 mM **CD-1**.

our catalytic system 2-naphthaldehyde would axially bind with **CD-1** in a way that the carbonyl group is amenable to noncovalent interaction with the appended chiral diamino group. The observed 7-fold larger binding constant of 2-naphthaldehyde over 1-naphthaldehyde is apparently in line with this binding mode. The opposite ICD signals between 1-naphthaldehyde and 2-naphthaldehyde in the presence of **CD-1** further proved the different orientation of the naphthaldehydes in the cavity. Moreover, the intenser ICD signal of 2-naphthaldehyde in **CD-1** solution reveals that the 2-naphthaldehyde extended more deeply via axial inclusion in the cavity of **CD-1** than 1-naphthaldehyde, which is bound in a much shallower equatorial orientation (Figure 10). The ROESY spectrum was next used to elucidate the detailed orientation of 2-naphthaldehyde in the cavity. 2-Naphthoic acid was chosen as an analogue for 2-naphthaldehyde because of its better solubility in aqueous solution and similar interactions with the diamine group of **CD-1**. The intense cross-peaks between  $\text{H1}'$ ,  $\text{H3}'$ , and  $\text{H4}'$  of 2-naphthoic acid and cyclodextrin inner protons  $\text{H3}$ ,  $\text{H5}$  define a detailed binding mode as depicted in Figure 11b. By analogue, 2-naphthaldehyde and **CD-1** would also form an axial inclusion with the aromatic ring partially extending out from the secondary rim of the CD cavity.

Meanwhile, some modest conformation changes of catalyst **CD-1** upon substrate binding have also been observed by

- (22) The relative ROESY intensities of CD derivatives can be utilized to determine conformation change in solution; for examples, see: (a) Alderfer, J. L.; Eliseev, A. V. *J. Org. Chem.* **1997**, *62*, 8225–8226. (b) Wenz, G.; Strassnig, C.; Thiele, C.; Engelke, A.; Morgenstern, B.; Hegetschweiler, K. *Chem.—Eur. J.* **2008**, *14*, 7202–7211. The ROESY cross-peak between  $\text{H12}^a$  and  $\text{H12}^e$  is set to 100 in both **CD-1** and **CD-2**. The ROESY intensity of selected relevant cross-peaks: **CD-1**: 82 ( $\text{H9}^a\text{--H9}^e$ ), 262 ( $\text{H10--H11}$ ), 17 ( $\text{H8--H5}$ ), 14 ( $\text{H9--H5}$ ); **CD-2**: 88 ( $\text{H9}^a\text{--H9}^e$ ), 266 ( $\text{H10--H11}$ ), 6 ( $\text{H8--H5}$ ), 6 ( $\text{H9--H5}$ ).
- (23) The molecular modeling was conducted using the CVFF force field in the Insight II/Discover program package (Accelrys Inc.) according to ref 19a. The energy minimum conformations of **CD-1** and **CD-2** in acidic buffer solution are in accordance with those proposed based on ROESY spectra. See Figure S5 in the Supporting Information for detailed data.
- (24) For examples, see: (a) Ikeda, H.; Nakamura, M.; Ise, N.; Oguma, N.; Nakamura, A.; Ikeda, T.; Toda, F.; Ueno, A. *J. Am. Chem. Soc.* **1996**, *118*, 10980–10988. (b) Ikeda, H.; Nakamura, M.; Ise, N.; Toda, F.; Ueno, A. *J. Org. Chem.* **1997**, *62*, 1411–1418.
- (25) (a) Blokzijl, W.; Engberts, J. B. F. N. *Angew. Chem., Int. Ed.* **1993**, *32*, 1545–1579. (b) Otto, S.; Engberts, J. B. F. N. *Org. Biomol. Chem.* **2003**, *1*, 2809–2820.

- (26) (a) Harata, K.; Uedaira, H. *Bull. Chem. Soc. Jpn.* **1975**, *48*, 375–378. (b) Shimizu, H.; Kaito, A.; Hatano, M. *Bull. Chem. Soc. Jpn.* **1979**, *52*, 2678–2684. (c) Shimizu, H.; Kaito, A.; Hatano, M. *Bull. Chem. Soc. Jpn.* **1981**, *54*, 513–519.
- (27) (a) Inoue, Y.; Hakushi, T.; Liu, Y.; Tong, L.-H.; Shen, B.-J.; Jin, D.-S. *J. Am. Chem. Soc.* **1993**, *115*, 475–481. (b) Nishijo, J.; Ushiroda, Y. *Chem. Pharm. Bull.* **1998**, *46*, 1790–1796.

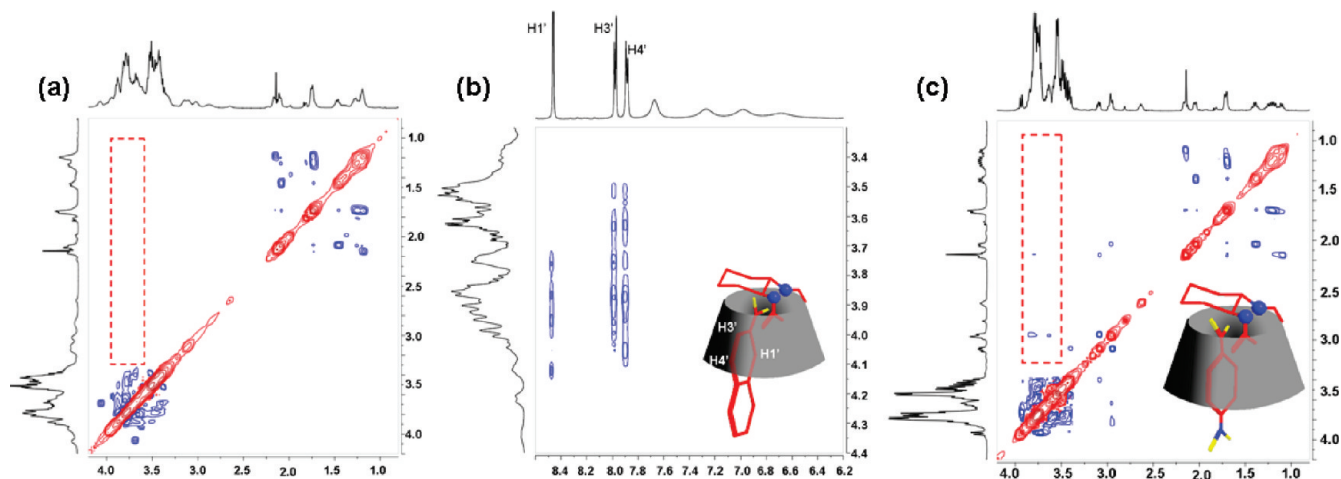
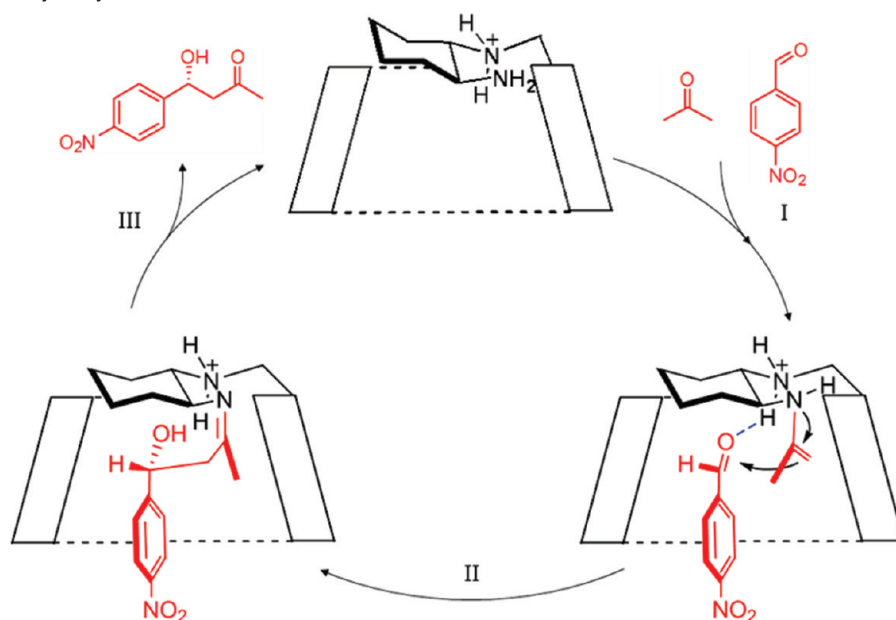


**Figure 11.** ROESY spectra of (a and b) **CD-1** (0.02 M) and 2-naphthoic acid (0.02 M) in acetate buffer (pH = 4.80, containing 2%  $d_6$ -acetone). (c) **CD-1** (0.02 M) and *p*-nitrobenzoic acid (0.02 M) in acetate buffer (pH = 4.80, containing 2%  $d_6$ -acetone).

**Scheme 3.** Proposed Catalytic Cycle



ROESY spectroscopy (Figure 11; also see Figure S9 in the Supporting Information for full ROESY spectrum). Upon treating **CD-1** with 2-naphthoic acid in the presence of acetone, analysis of ROESY spectrum (Figure 11a) suggests that the cyclohexyl ring is likely pushed out by the incoming naphthalene molecules as evidenced by much weakened NOE signals. A similar phenomenon has also been observed when *p*-nitrobenzoic acid was used as the binding substrate (Figure 11c). Considering that both 2-naphthoic acid and *p*-nitrobenzoic acid are competitive inhibitors for the studied reactions,<sup>28</sup> the proposed binding complexes as depicted in Figure 11 may reflect the ternary structure involved in the reaction coordinates.

**4.3. Proposed Catalytic Cycle.** On the basis of the data obtained from the binding studies and conformational analysis, we proposed the following catalytic cycle for the **CD-1** catalyzed asymmetric direct aldol reaction in aqueous buffer. The reaction

proceeds through roughly three stages (Scheme 3): (1) assembly of aldehyde and acetone donor in the **CD-1** cavity and enamine formation (**I**); (2) enamine addition to aldehyde, i.e. the C–C forming step (**II**); and (3) release of product from the cavity and regeneration of catalyst (**III**).

In a manner that closely parallels enzymatic catalysis, the substrate binding properties of our supramolecular catalyst **CD-1** have been unequivocally determined by separate binding studies with aldol acceptors (Table 3) and the obtained results are in good consistence with the well-known recognition behaviors of cyclodextrin derivatives. In our catalytic studies, a connection between the binding features with the corresponding catalytic behavior seems self-evident, where substrates with a poor binding ability normally resulted in low reactivity and stereoselectivity (Table 2). The major driving forces for the formation of a host–substrate complex can be ascribed to the ubiquitous hydrophobic interactions in cyclodextrin chemistry and noncovalent interactions of aldehyde with the appended diamino group in **CD-1** as proven in our substrate binding studies (Table 3). A control reaction in DMSO has also been examined to prove

(28) The aldol reactions of acetone and aromatic aldehydes (*p*-nitrobenzaldehyde and 2-naphthaldehyde) were ~2-fold slower when the corresponding aromatic acids were added to the system, whereas the enantioselectivity was maintained.

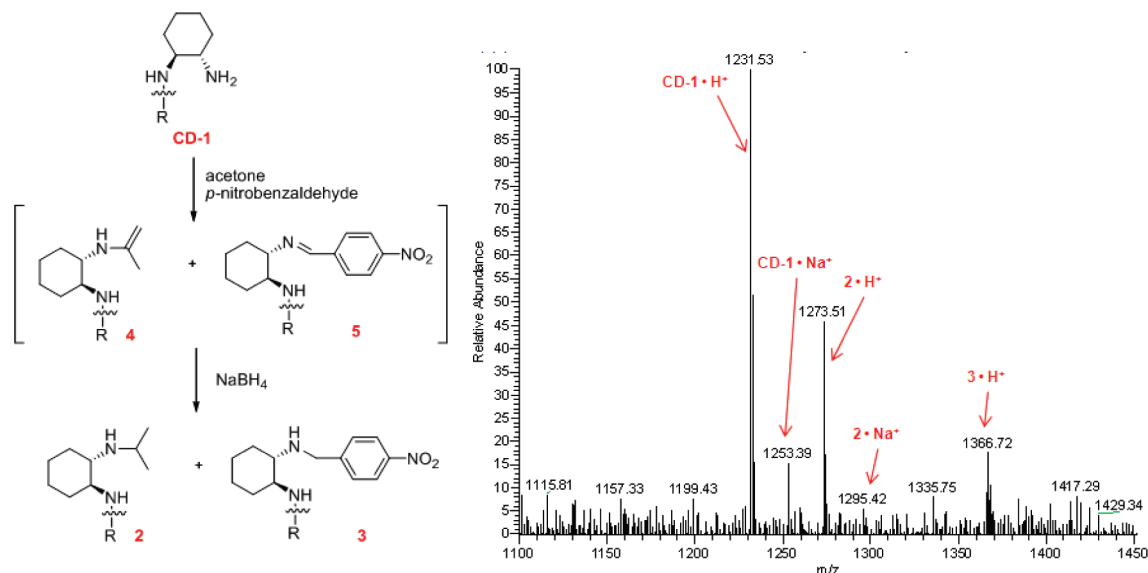


Figure 12. ESI-MS spectra of reaction mixture after treated with  $\text{NaBH}_4$ .

Table 4.  $k_{\text{obs}}$  of Deuteration of Aldol Donor<sup>a</sup>

Entry	Aldol donor	Cat	$k_{\text{obs}}$ ( $10^{-5} \text{ min}^{-1}$ )
1	Acetone	CD-1	3.49
2 <sup>b</sup>	Acetone	CD-1	5.30
3	Acetone	---	0.28
4	Cyclohexanone	CD-1	118
5	Cyclopentanone	CD-1	426

<sup>a</sup> Conditions: catalyst 0.02 M, aldol donor 0.1 M, 25 °C. Entries 1–3: 0.1 M acetate buffer (pH = 4.80). Entries 4–5: 0.1 M acetate buffer (pH = 4.80) containing 10% *d*<sub>6</sub>-DSMO. <sup>b</sup> *p*-Nitrobenzaldehyde was added to the system.

the involvement of cavity binding in the catalysis as the use of organic solvent was known to disfavor the encapsulation of a guest in the cyclodextrin cavity, which probably would lead to reaction inhibition. Indeed, the reaction was more than 16 times slower in DMSO than in acetate buffer ( $k_{\text{obs}} = 5.0 \times 10^{-5} \text{ mM/min}$  vs  $8.2 \times 10^{-4} \text{ mM/min}$ ). Additional inhibition experiments with aldehyde analogues such as *p*-nitrobenzoic acid and 2-naphthoic acid have also been examined, and only a very modest inhibition effect was observed in these cases,<sup>28</sup> indicating these acids are competitive inhibitors. Significant inhibition is only noticed with a much stronger cyclodextrin binder such as 2-bromoadamantane at high concentration (Table 1, entry 13). These observations together with the generally low binding constants suggest a highly dynamic and flexible guest binding and exchange in the current supramolecular catalysis and that a substrate binding pre-equilibrium precedes the rate-limiting step of the reaction.

Regarding aldol donor recognition, a dramatic size effect has been observed among a series of ketone donors examined. Only small ketones such as acetone, butanone, and cyclopentanone can be applied in CD-1 catalysis. Cyclohexanone, which is only one carbon different from cyclopentanone, reacted over 50 times slower in the presence of CD-1. With the observation that cyclohexanone demonstrates usually comparable or even better activity over cyclopentanone in asymmetric direct aldol reactions catalyzed by small molecular catalysts,<sup>29</sup> these results further

prove that the current supramolecular catalysis highly relies on the cyclodextrin cavity. In this instance, whether the complex of two substrates occurs sequentially or simultaneously may seem to have no bearing on catalysis, but in the deuteration experiments, we did observe that the deuteration of acetone is accelerated slightly in the presence of aldehyde (Table 4, entry 2 vs entry 1), suggesting that the binding of aldehyde has a direct impact on the enamine formation and pre-equilibrium assembly of substrates in the CD cavity might be allosteric and synergistic for subsequent catalysis.

Direct experimental evidence for the enamine mechanism was obtained from ESI-MS studies (Figure 12). The putative enamine intermediate **4** could be *in situ* trapped as isopropylated CD-1 ( $2 \cdot \text{H}^+$  in Figure 12) by treating the reaction mixture with  $\text{NaBH}_4$ . In addition, the background reaction in acetate buffer solution (pH = 4.80) without CD-1 has also been examined and no reaction was observed, excluding the possible enol pathway.

To characterize the rate-limiting step, the deuteration rate of  $\alpha$ -protons in acetone, which reflects closely the enamine formation rate, was next determined by  $^1\text{H}$  NMR.<sup>30,31</sup> In acetate buffer, CD-1 was found to catalyze the deuteration 12 times faster over the background exchange (Table 4, entry 1 vs 3). The deuteration catalyzed by CD-1 also followed Michaelis–Menten kinetics, showing a Lineweaver–Burk plot with a  $k_{\text{cat}} = 4.80 \times 10^{-3} \text{ min}^{-1}$ . From comparison of the  $k_{\text{cat}}$  of the overall reaction ( $6.07 \times 10^{-3} \text{ min}^{-1}$ ), the lower deuteration rate suggests the enamine-forming step might be, or at least partially be, the rate-limiting step in the current catalysis. Similar slower deuteration rates have also been observed with cyclohexanone and cyclopentanone donors. Again, it was noted that the deuteration of cyclohexanone was much slower (4-fold) than cyclopentanone,<sup>31</sup> further proving the cavity effect and the size selection in the catalysis of CD-1 (Table 4, entry 4 vs 5).

(29) In the presence of a small molecule catalyst such as **8**, the reaction of cyclohexanone is 3-fold faster than that of cyclopentanone. Details are presented in Table S3 in the Supporting Information.

(30) (a) Hine, J.; Mulders, J.; Houston, J. G.; Idoux, J. P. *J. Org. Chem.* **1967**, 32, 2205–2209. (b) Warkentin, J.; Tee, O. S. *J. Am. Chem. Soc.* **1966**, 88, 5540.

(31) In sharp contrast, the deuteration of cyclohexanone was  $\sim 3$  times faster than cyclopentanone when catalyzed by antibody aldolase according to Shulman, A.; Sitry, D.; Shulman, H.; Keinan, E. *Chem.–Eur. J.* **2002**, 8, 229–239.



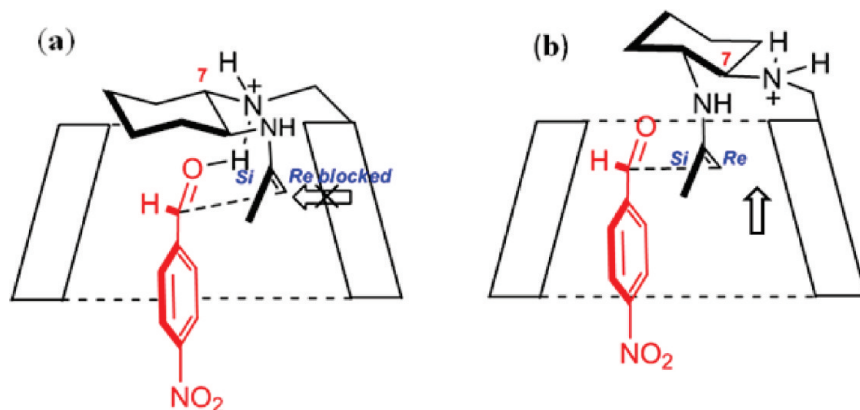
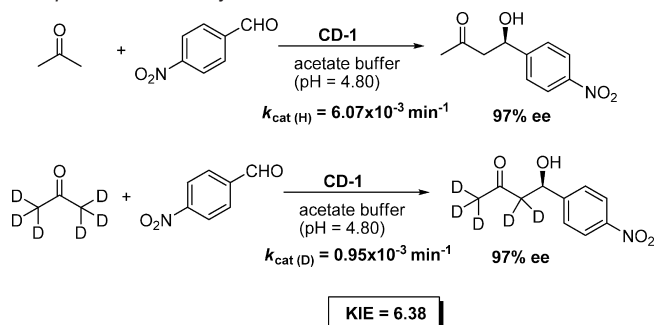


**Figure 13.** Proposed transition state of (a) **CD-1** and (b) **CD-2** catalyzed direct aldol reaction.

**Scheme 4.** Primary Isotope Effect in the Aldol Reaction of Acetone and *p*-Nitrobenzaldehyde



A convincing experiment that supports the enamine-forming step as the rate-limiting step is obtained from kinetic isotope experiments (Scheme 4). The primary kinetic hydrogen isotope effect was found in the aldol reaction of acetone and *p*-nitrobenzaldehyde ( $\text{KIE} = 6.38$ ). Note that the primary KIE was observed in the reaction with a different aldol acceptor 2-naphthaldehyde ( $\text{KIE} = 4.79$ ) and that with a different aldol donor cyclopentanone ( $\text{KIE} = 5.92$ ). The obtained significant primary KIE indicates that the rate-limiting step must involve C–H bond formation or cleavage, which apparently occurs only in the enamine-forming step in the aldol reactions.<sup>32</sup> The observation of a rate-limiting enamine-forming step stands in contrast to the well-known primary aminocatalysis in natural Type I aldolases, antibody aldolases, and organocatalyzed aldol reaction, where the C–C forming step is assumed as the rate-limiting step.<sup>6a,33</sup> However, rate-limiting enamine formation is not rare in enamine-based asymmetric catalysis. A rate-limiting enamine step was recently identified in the classical proline catalyzed Hajos–Parrish–Eder–Sauer–Wiechert reaction *via* theoretical calculation and <sup>13</sup>C KIE studies.<sup>34</sup> Accordingly, a rate-limiting enamine formation followed by product-determining C–C formation can be formulated in the current catalysis of **CD-1**. Presumably, the origin of a rate-limiting enamine step

can be ascribed to two factors: (1) the slightly acidic condition, which is overall beneficial for the current catalysis (Figure 3), may turn out to retard the enamine formation; note that most primary aminocatalysis in enzymes such as aldolase or decarboxylases occur favorably under neutral pH; (2) the assembly of two substrates in the CD cavity, i.e. aldol donor and acceptor, leading to proximity that facilitates C–C bond formation, results in overwhelming the enamine-forming step.

Upon forming the C–C bond, subsequent hydrolysis and release from the cavity (III) complete the catalytic cycle. The release of product from the cavity would be a quite kinetically facile process since we were unable to trap any product–**CD-1** conjugate under the reductive conditions (Figure 11). This observation, together with the generally low binding affinity of aldol products (Table 3), suggests that aldol products are not good guests for **CD-1** due to their large sizes and improper shapes, which well rationalizes the absence of product inhibitions in our supramolecular system.

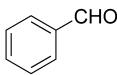
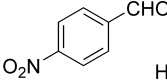
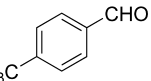
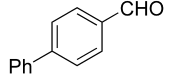
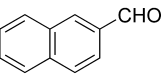
**5. Origin of Stereoselectivity: Cavity and Noncovalent Interactions.** Experimentally, we have observed that (1)  $\beta$ -cyclodextrin supported diamines, regardless of chirality and absolute configurations of the appended diamines, all gave *R*-stereoselective products and (2) **CD-1** with the configuration matched side chain demonstrated superior stereocontrol to its chirally unmatched analogue **CD-2**. These observations, combined with the binding features as well as the conformation analysis and molecular modeling, provide the basis for the transition state as depicted in Figure 13.

In this model, the chirality of cyclodextrin is imparted to the reactive enamine *via* a C<sub>6</sub>-connected diamino moiety, leading to differentiation of the *Re*- and *Si*-faces of the forming enamine, wherein the *Si*-face is more accessible in the rigid cyclodextrin cavity (Figure 13a). As summarized in Table 1, cyclodextrins appended with chiral diamines such as **CD-1**, **CD-2**, and **CD-3** all gave better (*R*)-enantioselectivity than **CD-4** endowed with an achiral diamine, a scenario where conformationally less flexible diamines induce more bias toward *Si*-face attack due to the constraint of the cyclodextrin cavity irrespective of the absolute configurations of side chains. Note that the stereoinductions with the supramolecular catalysts **CD-1** and **CD-2** are in sharp contrast to their small molecular analogues such as diamine **8**, where (*R*)-**8** and (*S*)-**8** gave (*R*)- and (*S*)-selective product, respectively. The uniformly observed (*R*)-selectivity as well as the dramatically improved enantioselectivity pinpoints the critical role of cyclodextrin cavity in channeling the stereoselective reaction pathway.

(32) In this scenario, the varied reaction rates with different aldehydes (Table 2) suggest that the binding of aldehyde may have a significant impact on the enamine formation. Our binding studies and the observation of the accelerated enamine formation in the presence of *p*-nitrobenzaldehyde (Table 4, entry 2) are clearly in line with this hypothesis. The elucidation of this unique feature awaits further studies.

(33) (a) Heine, A.; Desantis, G.; Luz, J. G.; Mitchell, M.; Wong, C.-H.; Wilson, I. A. *Science* **2001**, 294, 369–374. (b) Bahmanyar, S.; Houk, K. N. *J. Am. Chem. Soc.* **2001**, 123, 11273–11283.

(34) Zhu, H.; Clemente, F. R.; Houk, K. N.; Meyer, M. P. *J. Am. Chem. Soc.* **2009**, 131, 1632–1633.

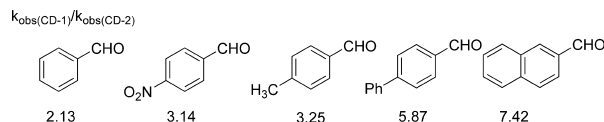
Aldol Acceptor					
$ee_{CD-1}$ (%)	91	97	92	99	97
$ee_{CD-2}$ (%)	45	68	67	95	90

**Figure 14.** Size effect of aldehyde acceptors in the aldol reactions of acetone.

The inferior stereocontrol with **CD-2** can also be explained by considering a similar model (Figure 13b). In comparison with **CD-1**, the *re*- and *si*-faces of the forming enamine becomes less differentiated in the **CD-2** cavity due to the excluded side chains as well as the unfavorable orientation of the primary amine moiety and hence both faces are accessible, causing low enantioselectivity. Based on this model, the use of a larger substrate would induce more bias toward *si*-face attack, leading to better stereoselectivity when catalyzed by **CD-2**. The observation of improved enantioselectivity with increasing acceptor size is clearly in line with this hypothesis (Figure 14). For example, by switching the acceptor from the smaller benzaldehyde to the relatively larger 4-toluenaldehyde and 4-phenylbenzaldehyde, the enantioselectivity was increased from 45% to 95% *ee* (Figure 14). Since the electronic nature is significantly varied in this series of aldehydes, the size effect would be the major contributor in this context. Indeed, a good linear correlation between Charton steric parameters and the log of *e.r.* is observed in the **CD-2** catalyzed system.<sup>35</sup> On the other hand, the changes in substrates barely influence the stereoselectivity when it comes to **CD-1**, suggesting a favorable cavity setting in balance with other interacting factors such as noncovalent interactions with the side chain is reached in this case.<sup>36</sup>

In addition to the chiral cavity, noncovalent interactions, particularly those involving the protonated amino group, would also play significant roles in the asymmetric catalysis by first assisting in assembling the substrates in the cavity as we have already discussed above, followed by stabilizing the transition state, e.g. via hydrogen bonding with the carbonyl group, to achieve better stereocontrol as shown in Figure 13. In this regard, the unfavorable noncovalent interactions (Figure 13b) with the suspended side chain in **CD-2** would also account for the generally low catalytic activity and enantioselectivity.

- (35) See Figure S6 in the Supporting Information for details. The value of Charton steric parameters is according to Charton, M., Motoc, I., Eds.; *Steric Effects in Drug Design*; Springer: Berlin, 1983; pp 68–75.
- (36) Despite a favorable size effect on enantioselectivity in the catalysis of **CD-2**, there are negative impacts on the reaction rate and the catalytic rate difference between **CD-1** and **CD-2** for the same reaction was found to increase linearly with the increasing size of the substrates, suggesting that other interactions such as noncovalent interactions with a protonated side chain ammonium group should play critical roles for effective catalysis besides the cavity effect.



Though we were unable to directly characterize these noncovalent interactions under acetate buffer conditions, the pH profiles of **CD-1** catalysis are clearly in accordance with the proposal that protonated amino groups are involved in the noncovalent interactions as well-established in enamine-based small molecular catalysis using chiral diamine–Bronsted acid conjugates;<sup>7a–c,m,37</sup> note that the stereoselectivity is totally depleted when the pH was increased over 6.5.

## Conclusion

In conclusion, asymmetric supramolecular primary amine catalysts have been evolved by covalently connecting relevant organocatalysts with a cyclodextrin host, illustrating a viable approach for the development of asymmetric supramolecular catalysts. **CD-1** is found to be a remarkable asymmetric supramolecular aldol catalyst that works effectively in aqueous acetate buffer solution (pH = 4.80) with high activity and stereoselectivity. In a manner closely resembling enzymatic catalysis, **CD-1** selectively binds and situates substrates in the reactive cavity by the synergistic action of a hydrophobic effect and noncovalent interactions with a protonated diamino side chain. The reaction proceeds through a rate-limiting enamine formation step followed by product-determining C–C formation. Hydrolytic release of the product from the cavity completes the cycle, and no product inhibition has been observed. Unlike enzymatic primary aminocatalysis, **CD-1** works much more favorably under slightly acidic conditions rather than enzymatic neutral conditions, a distinctive feature that is also characteristic of small molecular amino catalysts with protonated amino groups as hydrogen-bonding catalytic motifs.<sup>7a–c,m,37</sup> Collectively, **CD-1** represents a rare example that merges an organocatalytic motif with supramolecular principles, leading to an asymmetric supramolecular catalyst with synthetic applicability, meanwhile, providing insights into enzymatic catalysis.

**Acknowledgment.** This work was supported by the Natural Science Foundation of China (NSFC 20702052 and 20972163), the Ministry of Science and Technology (MoST) (2008CB617501, 2009ZX09501-018), and the Chinese Academy of Sciences. We thank Prof. Judith Klinman and Prof. Qiyu Zheng for helpful discussions.

**Supporting Information Available:** Detailed experimental procedures and product characterization. This material is available free of charge via the Internet at <http://pubs.acs.org>.

JA102819G

- (37) Saito, S.; Yamamoto, H. *Acc. Chem. Res.* **2004**, *37*, 570–579.